










Morphometric analysis of the internal auditory canal and its clinical-surgical implications

Análise morfométrica do meato acústico interno e suas implicações clínico-cirúrgicas



Fernando Augusto Pacífico¹  Bárbara Belijane Adriano Leonel¹ 
Bruno Peixoto Gonçalves¹  Juliana Natalie Rodrigues Marques¹ 
Darllan Rocha Barros¹  Thiago José Monteiro Borges da Silva Valente¹ 
Ismael Felipe Gonçalves Galvão¹ 

¹ Faculdade de Medicina de Olinda. Olinda, Pernambuco, Brazil.

Abstract

Introduction: The internal auditory canal (IAC) is a short and narrow bone canal close to some bone openings, such as the jugular foramen, allowing the passage of important structures. **Objective:** To assess the morphometric measures of the IAC in human skulls, analyse its microanatomy, and elucidate clinical-surgical implications associated with this canal. **Methods:** This cross-sectional, descriptive, and comparative study analysed 30 human skulls regardless of sex, age, or ancestry. Statistical analysis was conducted using SPSS software. **Results:** The vertical diameter of the IAC was 3.5 ± 0.92 mm in the right antimerere (RA) and 3.7 ± 0.92 mm in the left antimerere (LA), while the horizontal diameter was 4.8 ± 1.01 mm in the RA and 4.6 ± 1.20 mm in the LA. The upper length of the IAC was 10.3 ± 1.76 mm in the RA and 10.40 ± 1.56 mm in the LA, while the lower length was 9.1 ± 1.72 mm in the RA and 9.6 ± 1.54 mm in the LA. **Conclusions:** The right and left antimeres showed significant differences in three specific variables: upper length of the IAC, distance from the lateral or external edge of the IAC to the groove of the sigmoid sinus, and distance from the lateral or external edge of the IAC to the external opening of the vestibular aqueduct.

Keywords: Anatomy; Anthropometry; Ear canal; Temporal bone.

How to cite: Pacífico **FA**, Leonel **BBA**, Gonçalves **BP**, Marques **JNR**, Barros **DR**, Valente **TJMBS**, et al. Morphometric analysis of the internal auditory canal and its clinical-surgical implications. *An Fac Med Olinda* 2024; 1(12):33 doi: <https://doi.org/10.56102/afmo.2024.352>

Corresponding author:

Fernando Augusto Pacífico

E-mail: fapacifico@outlook.com

Funding: Not applicable.

Research ethics

committee: no. 5689062

Received in 02/23/2024

Approved in 09/02/2024

Resumo

Introdução: O meato acústico interno (MAI) é um canal ósseo curto e estreito próximo a algumas aberturas ósseas, como o forame jugular, e que dá passagem a estruturas importantes. **Objetivo:** Avaliar as medidas morfométricas do MAI em crânios humanos secos, proporcionar uma análise detalhada da microanatomia da região e elucidar as implicações clínico-cirúrgicas associadas ao canal. **Métodos:** Trata-se de um estudo transversal e descritivo comparativo no qual foram analisados 30 crânios humanos, sem distinção de sexo, idade e ancestralidade. A análise estatística foi conduzida utilizando o software SPSS. **Resultados:** O diâmetro vertical do MAI foi $3,5 \pm 0,92$ mm no antímero direito (AD) e $3,7 \pm 0,92$ mm, no antímero esquerdo (AE). O diâmetro horizontal do MAI foi $4,8 \pm 1,01$ mm no AD e $4,6 \pm 1,20$ mm no AE. O comprimento superior do MAI foi $10,3 \pm 1,76$ mm no AD e $10,4 \pm 1,56$ mm no AE. O comprimento inferior do MAI foi $9,1 \pm 1,72$ mm no AD e $9,6 \pm 1,54$ mm no AE. **Conclusões:** Foram encontradas diferenças estatisticamente significativas entre os lados direito e esquerdo em três variáveis específicas: o comprimento superior do MAI, a distância da borda lateral ou externa do MAI até o seio do sulco sigmoide e a distância da borda lateral ou externa do MAI até a abertura externa do aqueduto vestibular.

Palavras-chave: Anatomia, Antropometria, Meato acústico; Osso temporal.

INTRODUCTION

The internal auditory canal (IAC) is a short and narrow bone canal located approximately one centimeter from the internal part of the temporal bone and closed by a thin perforated bone plate that separates it from the inner ear¹. Also, the IAC is close to bone openings (e.g., jugular foramen) and allows the passage of important structures, such as the facial and vestibulocochlear nerves (VII and VIII nerves, respectively), labyrinthine artery, and vestibular ganglion, which are crucial for the auditory and vestibular systems^{1,2}.

The VII pair innervates the facial mimicry, stapedius, stylohyoid, and posterior belly of the digastric muscles through a motor root forming the nerve^{3,4}. The nervus intermedius (also known as intermediate nerve of Wrisberg) is the sensitive and visceral root responsible for innervating the lacrimal, submandibular, and sublingual glands, controlling the production of tears and saliva^{3,4}. It also conducts the taste to the anterior two-thirds of the tongue and provides sensibility to part of the external ear, ear canal, and posterior areas of the nasal cavities and soft palate^{3,4}. The vestibular portion of the VIII pair influences the ocular and cephalic movements and trunk and limb muscles, contributing to the maintenance of balance, while the cochlear portion is responsible for hearing sensitivity^{3,4}.

Clinically, the IAC has structural relevance in forming cavernous angiomas, neuromas, malformations, or cavernomas, which may influence the functions of the related cranial nerves^{3,4}.

Considering the advances in endoscopic surgery and microsurgery, the topographic study associating cranial nerves with IAC has been impacting the understanding of possible anatomic variations and their clinical implications^{5,6}. Some studies observed variations in the length, width, and shape (e.g., funnel, cylindrical, or round), and these parameters are important for the safety and efficacy of the surgical procedures involving the IAC^{5,6}.

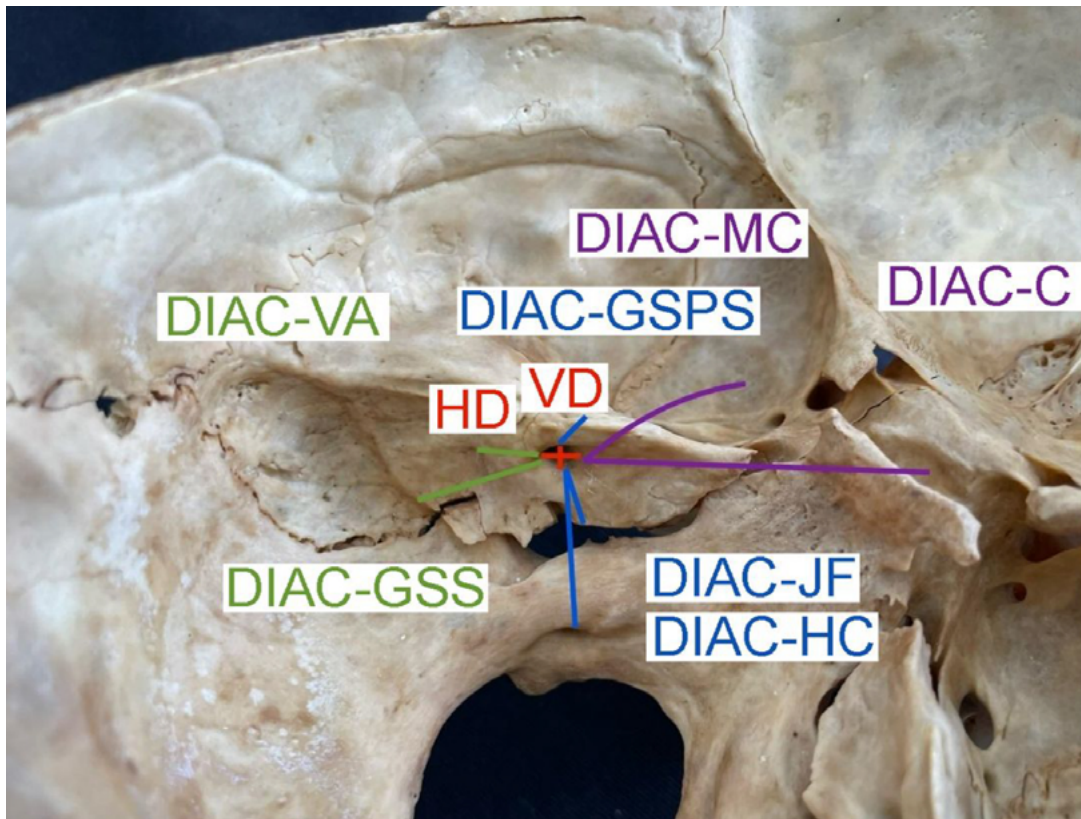
Despite the current evidence, a lack of data was observed in literature regarding the morphometric assessment of the IAC in human skulls and their distances from the adjacent structures. Thus, the present study aimed to assess the morphometric measures of the IAC in human skulls, providing a detailed analysis of its microanatomy and elucidating the clinical-surgical implications associated with this canal.

METHODS

This cross-sectional, comparative, and descriptive study analysed 30 human skulls (60 cm) regardless of sex, age, or ancestry from cadaveric pieces of a higher education institution using a non-probability and convenience sampling. All damaged skulls were excluded from the study, and both antimeres were analysed to measure the variables.

The present study was organized into two steps: morphologic classification and morphometric measures. Regarding the morphometric measures, the following parameters (Figures 1 and 2) were obtained in the right and left antimeres using a Castroviejo-type curved dry-point compass and a caliper:

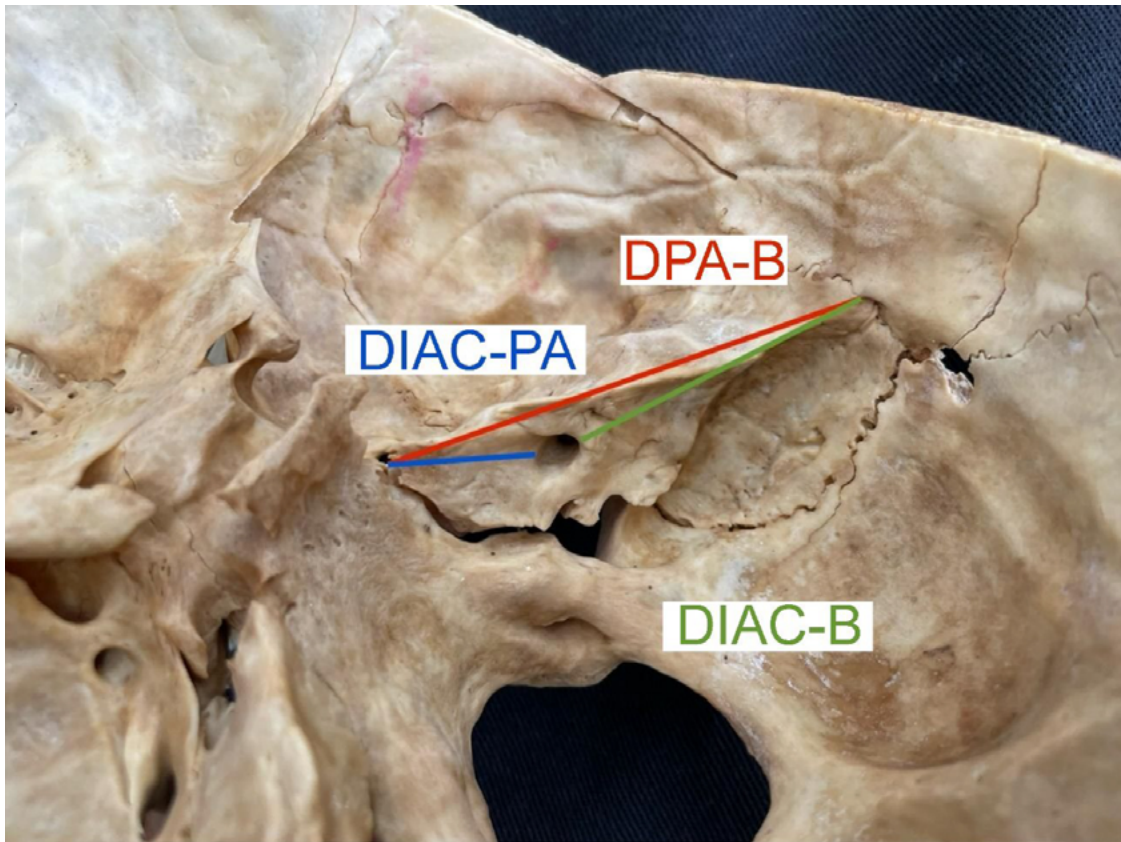
Figure 1. Superomedial view of the left temporal bone showing the morphometric measures.



VD: vertical diameter of the internal auditory canal (IAC); HD: horizontal diameter of the IAC; DIAC-JF: distance between the IAC and jugular foramen; DIAC-HC: distance between the IAC and hypoglossal canal; DIAC-GSPS: distance between the IAC and groove for the superior petrosal sinus; DIAC-gSS: distance between the IAC and groove of the sigmoid sinus; DIAC-VA: distance between the IAC and vestibular aqueduct; DIAC-C: distance between the PAI and clivus; DIAC-MC: distance between the PAI and Meckel's cave.

1. VD: vertical diameter (superior-inferior or dorsoventral) of the internal auditory canal (IAC);
2. HD: horizontal diameter (anteroposterior or rostral-caudal) of the IAC;
3. Upper length of the IAC: distance from the superior margin of the IAC to the most lateral point at the bottom in the region of the cribriform plate for the superior vestibular nerve;
4. Lower length of the IAC: distance from the inferior margin of the IAC to the most lateral point at the bottom in the region of the cribriform plate for the inferior vestibular nerve;
5. DIAC-JF: distance between the inferior edge of the IAC and jugular foramen (jugular notch of the temporal bone);
6. DIAC-HC: distance from the inferior edge of the IAC to the hypoglossal canal;
7. DIAC-GSPS: distance from the superior edge of the IAC to the groove for the superior petrosal sinus (superior edge of the petrosal triangle);
8. DIAC-GSS: distance from the lateral or external edge of the IAC to the groove of the sigmoid sinus;
9. DIAC-VA: distance from the lateral or external edge of the IAC to the external opening of the vestibular aqueduct;
10. DIAC-C: distance from the medial or internal edge of the IAC to the clivus;
11. DIAC-MC: distance from the medial or internal edge of the IAC to the Meckel's cave;
12. DPA-B: distance from the petrous apex to the base of the petrous part of the temporal bone;
13. DIAC-PA: distance from the medial or internal edge of the IAC to the petrous apex;
14. DIAC-B: distance from the lateral or external edge of the IAC to the base of the intracranial petrous part of the temporal bone.

Figure 2. Superomedial view of the right temporal bone showing morphometric measures.



DPA-B: distance between the petrous apex and base of the petrous part of the temporal bone; DIAC-PA: distance between the internal auditory canal (IAC) and petrous apex; DIAC-B: distance between the IAC and base of the petrous part of the temporal bone.

The format of the IAC was observed as a non-morphometric parameter, which can be classified as type I to VI, according to Unur *et al.* (2007):

Type I: round

Type II: oval

Type III: U-shaped

Type IV: fissure

Type V: irregular

Type VI: V-shaped

The SPSS® software (IBM Corp., Chicago, EUA) was used for statistical analyses. The paired *t*-test was used for comparison between means, and statistical significance was set at $p < 0.05$.

RESULTS

Table 1 presents the results of measures and variations. VD varied from 1.5 to 5.5 mm (3.50 ± 0.92 mm) in the right antimeres and from 2.50 to 5.50 mm (3.70 ± 0.92 mm) in the left antimeres, while the HD varied from 3 to 7.50 mm (4.80 ± 1.01 mm) in the right antimeres and from 2 to 8.50 mm (4.60 ± 1.20 mm) in the left antimeres. The upper length of the IAC varied from 8 to 15 mm (10.30 ± 1.76 mm) in the right antimeres and from 8 to 14 mm (10.40 ± 1.56 mm) in the left antimeres, while the lower length varied from 6 to 13 mm (9.10 ± 1.72 mm) in the right antimeres and from 7 to 12 mm (9.60 ± 1.54 mm) in the left antimeres.

Table 1. Comparison of diameters, lengths, and distances of the IAC in the right and left antimeres.

Measure	Right antimeres (mean \pm SD)	Left antimeres (mean \pm SD)	t-test	p-value
VD	3.5 ± 0.92	3.7 ± 0.92	-1.507	0.143
HD	4.8 ± 1.01	4.6 ± 1.20	1.718	0.097
ULIAC	10.3 ± 1.76	10.4 ± 1.56	-0.571	0.573
LLIAC	9.1 ± 1.72	9.6 ± 1.54	-2.151	0.040*
DIAC-JF	6.2 ± 1.36	6.5 ± 1.36	-1.730	0.094
DIAC-HC	19.7 ± 2.38	19.5 ± 2.42	1.101	0.280
DIAC-GSPS	4.8 ± 0.90	4.6 ± 1.03	1.087	0.286
DIAC-GSS	22.1 ± 2.46	23.4 ± 2.46	-3.060	0.005*
DIAC-VA	10.2 ± 2.49	11.3 ± 2.55	-2.488	0.019*
DIAC-C	35.8 ± 2.96	35.1 ± 2.78	1.287	0.208
DIAC-MC	32.5 ± 3.39	31.9 ± 2.66	1.357	0.185
DPA-B	57.0 ± 4.02	56.1 ± 4.20	1.766	0.088
DIAC-PA	19.2 ± 2.93	18.7 ± 2.68	1.438	0.161
DIAC-B	35.9 ± 3.23	34.8 ± 3.91	1.994	0.056

* Statistically significant ($p < 0.05$) – t-test.

VD: vertical diameter of the internal auditory canal (IAC); HD: horizontal diameter of the IAC; ULIAC: upper length of the IAC; LLIAC: lower length of the IAC; DIAC-JF: distance between the IAC and jugular foramen; DIAC-HC: distance between the IAC and hypoglossal canal; DIAC-GSPS: distance between the IAC and groove for the superior petrous sinus; DIAC-GSS: distance between the IAC and groove of the sigmoid sinus; DIAC-VA: distance between the IAC and vestibular aqueduct; DIAC-C: distance between the IAC and clivus; DIAC-MC: distance between the IAC and Meckel's cave; DPA-B: distance between the petrous apex and base of the petrous part of the temporal bone; DIAC-PA: distance between the IAC and petrous apex; DIAC-B: distance between the IAC and the base of the petrous part of the temporal bone; SD: standard deviation.

The following measures were obtained in the antimeres: DIAC-JF varied from 4 to 9.5 mm (6.20 ± 1.36 mm) in the right and from 4 to 9.5 mm (6.50 ± 1.36 mm) in the left; DIAC-HC varied from 14.5 to 24.5 mm (19.7 ± 2.38 mm) in the right and from 15 to 24 mm (19.5 ± 2.42 mm) in the left; DIAC-GSPS varied from 2.5 to 6.5 mm (4.80 ± 0.90 mm) in the right and from 2.5 to 6.5 mm (4.60 ± 1.03 mm) in the left; DIAC-GSS varied from 16.50 to 28 mm (22.10 ± 2.46 mm) in the right and from 17 to 28.50 mm (23.40 ± 2.46 mm) in the left; DIAC-VA varied from 7 to 18.5 mm (10.20 ± 2.49 mm) in the right and from 7.5 to 17 mm (11.30 ± 2.55 mm) in the left; DIAC-C varied from 29.50 to 41.5 mm (35.80 ± 2.96 mm) in the right and from 30 to 40.5 mm (35.10 ± 2.78 mm) in the left; DIAC-MC varied from 25 to 37.5 mm (32.50 ± 3.39 mm) in the right and from 28 to 37 mm (31.90 ± 2.66 mm) in the left; DPA-B varied from 46 to 66 mm (57 ± 4.02 mm) in the right and from 48 to 64 mm (56.10 ± 4.20 mm) in the left; DIAC-PA: varied from 12 to 24.50 mm (19.20 ± 2.93 mm) in the right and from 11 to 23 mm (18.70 ± 2.68 mm) in the left; and DIAC-B varied from 27 to 42 mm (35.90 ± 3.23 mm) in the right and from 25.50 to 42 mm (34.80 ± 3.91 mm) in the left.

A comparative analysis of the diameters, lengths, and distances was performed on both antimeres using the paired *t*-test, and the results are presented in Table 1 as mean and standard deviation. Significant differences between the right and left antimeres were observed in three specific variables: upper length of the IAC, DIAP-GSS, and DIAP-VA.

The most common type of IAC was the oval, present in 36.6% ($n = 22$) of all temporal bones, followed by the round, found in 30% ($n = 18$). The oval type was the most common in the right IAC, corresponding to 44.3% ($n = 13$), while the oval and round types showed the same frequency in the left IAP, with 3% each ($n = 9$). The irregular (i.e., the least common) type was not observed in temporal bones.

DISCUSSION

Considering the embryological aspect, the IAC is developed from the chondrification and ossification of the mesodermal layer, which surrounds the VII and VIII nerves at the petrous part of the temporal bone in the posterior cranial fossa^{2,7}. Although the IAC lengthens as the skull increases in size until approximately ten years old, the diameter of the medial opening only increases slightly during the first year of life².

Most individuals present only one canal; however, literature describes approximately 21 rare cases of doubled IAC associated with inner ear malformations and frequently related to stenosis in this region⁷. Thus, an adequate morphometric assessment of the IAC is essential to develop a database related to the anatomy of intracranial pathologies. It may also support microsurgery techniques to approach the cerebellopontine angle and vestibular schwannoma, enhancing the protection of the related structures (e.g., inner ear and VII and VIII nerves)⁸.

The assessment of anatomical patterns of the IAC may determine the need for a surgical

approach⁸ in specific conditions, such as congenital abnormalities, cranial trauma, and peripheral nerves and ear pathologies. The IAC measures also indicate pathologies (e.g., tumors and stenosis), confirming the relevance of its morphometry in both antimeres⁸. Also, literature has described regional and ethnic aspects and variations between antimeres as factors for morphometric differences of the IAC⁸.

A study using high-resolution computed tomography in 128 patients (83 with inner ear malformations and 45 without changes) showed a mean diameter of the IAC of approximately 5.5 mm, corroborating the left antimeres of the present study, but higher than the diameter observed in the right antimeres⁹. A measure of approximately 2 mm width is considered adequate for a neurovascular bundle, and a smaller diameter indicates a narrow canal related to aplasia of the cochlear portion of the VIII nerve and congenital sensorineural hearing loss. Also, studies reported that a difference > 2 mm in the diameter between IAC antimeres might be a tumor marker^{1,6,9}. The largest left HD found in this study was 8.5 mm; a diameter > 8 mm is considered enlarged and may be associated with tumors, such as vestibular schwannomas and facial neuromas (less frequent)^{6,10}.

A retrospective study with 142 healthy individuals (18 to 60 years old) showed that the mean length of IAC was 9.71 mm (right) and 9.92 mm (left), and the diameter was 3.97 mm (right) and 3.95 mm (left), corroborating the present study. Differences in the IAC morphometry may be due to ethnic and regional aspects and variations between antimeres, and a study reported a difference related to sex, which is still unclear¹.

The morphometric data of the IAC are important to assess patients with pathologies in this region, such as vestibular schwannoma (i.e., the most common tumor), due to its proximity with the cerebellopontine angle². Although benign, vestibular schwannomas may cause microvascular compression in the VII and VIII nerves, leading to tinnitus, vertigo, and hemifacial spasms. Also, these tumors present a high potential to expand to the cerebellopontine angle^{2,11}, and the retrosigmoid approach is indicated in these cases. However, the unawareness of the morphometry of IAC and related structures may cause injuries on the anterior inferior cerebellar artery and VII, IX, and X nerves⁸.

Understanding the IAC parameters and orientation and position in the petrous part of the temporal bone is important for translabyrinthine approaches since the unawareness of these data may lead to VII nerve injury¹². The diameter and length are also relevant for the most recent approaches, such as the minimally invasive transcanal transpromontorial through the external ear canal¹³. In addition, the morphometry of the IAC supports the understanding of its development in pediatric patients, ensuring safety in procedures involving this region¹².

Considering the relevance of morphometric data of the IAC, procedures involving this region have become safer. This is mainly due to the advance of imaging exams associated with en-

doscopic techniques through the canal, especially through the middle cranial fossa by the Fisch approach, which has been improved and performed since 1970¹⁴.

CONCLUSION

The present study found differences between the right and left antimeres in three specific variables: mean upper length of the IAC (10.30 and 10.40 mm in the right and left, respectively); DIAC-GSS (22.10 and 23.40 mm in the right and left, respectively); and DIAC-VA (10.20 and 11.30 mm in the right and left, respectively). These findings highlighted the anatomical characteristics between the antimeres of IAC, and the discrepancies should be considered when interpreting results and planning clinical interventions.

CONFLICTS OF INTEREST

The authors declare no conflicts of interest.

AUTHOR CONTRIBUTIONS

FAP - conceptualization, data curation, investigation, methodology, project management, resources, supervision, writing (initial manuscript), revision, and edition; **BBAL** - investigation, writing (initial manuscript), revision, and edition; **BPG** – investigation and writing (initial manuscript); **JNRM** - data curation, investigation, writing (initial manuscript), revision, and edition; **DRB** - investigation, writing (initial manuscript), revision, and edition; **TJMBSV** – supervision, writing (initial manuscript), revision, and edition; and **IFGG** - supervision, writing (initial manuscript), revision, and edition. All authors approved the final version to be published.

REFERENCES

1. Özandaç Polat S, Uygur AG, Öksüzler FY, Öksüzler M, Yücel AH. Morphometric measurements of the internal acoustic meatus. *Cukurova Med J.* 2019;44:419-26. <https://doi.org/10.17826/cumj.565954>
2. Panara K, Hoffer M. Anatomy, Head and Neck, Ear Internal Auditory Canal (Internal Auditory Meatus, Internal Acoustic Canal). In: StatPearls. Treasure Island (FL): StatPearls Publishing; 2022 Aug 29. PMID: 31335008. Available in: <https://www.ncbi.nlm.nih.gov/books/NBK544288/>
3. Neto AH, Olivieri BV, Nascimento PA, Henrique S, Tucunduva MJA. Avaliação das Dimensões do Meato Acústico Interno em Tomografia Computadorizada Helicoidal. *Science in Health*, jan-abr 2016; 7(1)16-21. Disponível em: https://arquivos.cruzeirodosuleducacional.edu.br/principal/new/revista_scienceinhealth/19_jan_abr_2016/Science_07_01_16-21.pdf
4. Hovland N, Phuong A, Lu GN. Anatomy of the facial nerve. *Operative Techniques in Otolaryngology-Head and Neck Surgery.* 2021 Dec;32(4):190-6. <https://doi.org/10.1016/j.j>

otot.2021.10.009

5. Mandato Ferragut J, Azevedo Randi B, Américo Lourenço E, José Caldeira E, , Minatel E. Avaliação anatômica do diâmetro do poro acústico interno e suas correlações clínicas. *Perspectivas Médicas* [Internet]. 2008;19(2):16-18. Recuperado de: <https://www.redalyc.org/articulo.oa?id=243217620005>
6. Mntungwa N, Human-Baron R, Hanekom T. Morphology of the internal auditory canal: Deriving parameters from computer tomography scans. An observational STROBE-MR study. *Ear Nose Throat J*. 2022 Aug 13;1455613221116196. <https://doi.org/10.1177/01455613221116196>
7. Manchanda S, Bhalla AS, Kumar R, Kairo AK. Duplication Anomalies of the Internal Auditory Canal: Varied Spectrum. *Indian J Otolaryngol Head Neck Surg*. 2019 Sep;71(3):294-298. doi: <https://doi.org/10.1007/s12070-017-1087-4>
8. Akın-Saygin D, Nur-Türkoglu F, Aydin-Kabakçı AD, Alpa S. Internal Acoustic Opening: Different Osseous Landmarks and their Clinical Implications. *Int J Morphol*. 2022;40(5):1368-75. doi: <https://doi.org/10.4067/S0717-95022022000501368> .
9. Bächinger D, Breitsprecher TM, Pscheidl A, Dhanasingh A, Mlynski R, Dazert S, Langner S, Weiss NM. Internal auditory canal volume in normal and malformed inner ears. *Eur Arch Otorhinolaryngol*. 2023 May;280(5):2149-2154. doi: <https://doi.org/10.1007/s00405-022-07676-1> . Epub 2022 Oct 9. PMID: 36210370; PMCID: PMC10066105.
10. Stimmer H, Niedermeyer HP, Kehl V, Rummeny EJ. Nontumorous Enlargement of the Internal Auditory Canal: A Risk Factor for Sensorineural Hearing Loss? A High Resolution CT-Study. *Rofo*. 2015 Jun;187(6):450-8. doi: <https://doi.org/10.1055/s-0034-1399009> . Epub 2015 Apr 23. PMID: 25905691.
11. Ramly NA, Roslenda AR, Suraya A, Asma A. Vascular loop in the cerebellopontine angle causing pulsatile tinnitus and headache: a case report. *EXCLI J*. 2014 Feb 27;13:192-6. PMID: 26417253; PMCID: PMC4464511. <https://pmc.ncbi.nlm.nih.gov/articles/PMC4464511/>
12. Rennert RC, Brandel MG, Steinberg JA, Friedman RA, Couldwell WT, Fukushima T, Day JD, Khalessi AA, Levy ML. Maturation of the internal auditory canal and posterior petrous bone with relevance to lateral and posterolateral skull base approaches. *Sci Rep*. 2022 Mar 3;12(1):3489. doi: <https://doi.org/10.1038/s41598-022-07343-9> . PMID: 35241717; PMCID: PMC8894491.
13. Presutti L, et al. Expanded transcanal transpromontorial approach to the internal auditory canal: Pilot clinical experience. *Laryngoscope*. 2017;127:2608–2614. doi: <https://doi.org/10.1002/lary.26559>
14. Guo Y, Li M, Cheng K, Li Y, Ma Q. Three-dimensional imaging for the localization of related anatomical structures during surgery on the internal auditory canal. *BMC Surg*. 2022 Mar 2;22(1):74. doi: <https://doi.org/10.1186/s12893-022-01527-w>